White matter disruption in moderate/severe pediatric traumatic brain injury: Advanced tract-based analyses

Emily L. Dennis[a], Yan Jin[a], Julio E. Villalon-Reina[a], Liang Zhan[a], Claudia L. Kernan[b], Talin Babikian[b], Richard B. Mink[c], Christopher J. Babbitt[d], Jeffrey L. Johnson[e], Christopher C. Giza[f], Paul M. Thompson[a,g,*], Robert F. Asarnow[b,h]

[a]Imaging Genetics Center, Institute for Neuroimaging and Informatics, USC Keck School of Medicine, Los Angeles, CA, USA
[b]Department of Psychiatry and Biobehavioral Sciences, Semel Institute for Neuroscience and Human Behavior, UCLA, Los Angeles, CA, USA
[c]Department of Pediatrics, Harbor-UCLA Medical Center and Los Angeles BioMedical Research Institute, Torrance, CA, USA
[d]Department of Pediatrics, Miller Children's Hospital, Long Beach, CA, USA
[e]LAC + USC Medical Center, Department of Pediatrics, Los Angeles, CA, USA
[f]Dept of Neurosurgery and Division of Pediatric Neurology, UCLA Brain Injury Research Center, Mattel Children's Hospital, Los Angeles, CA, USA
[g]Departments of Neurology, Pediatrics, Psychiatry, Radiology, Engineering, and Ophthalmology, USC, Los Angeles, CA, USA
[h]Department of Psychology, UCLA, Los Angeles, CA, USA

ARTICLE INFO

ABSTRACT

Traumatic brain injury (TBI) is the leading cause of death and disability in children and can lead to a wide range of impairments. Brain imaging methods such as DTI (diffusion tensor imaging) are uniquely sensitive to the white matter (WM) damage that is common in TBI. However, higher-level analyses using tractography are complicated by the damage and decreased FA (fractional anisotropy) characteristic of TBI, which can result in premature tract endings. We used the newly developed autoMATE (automated multi-atlas tract extraction) method to identify differences in WM integrity. 63 pediatric patients aged 8–19 years with moderate/severe TBI were examined with cross sectional scanning at one or two time points after injury: a post-acute assessment 1–5 months post-injury and a chronic assessment 13–19 months post-injury. A battery of cognitive function tests was performed in the same time periods. 56 children were examined in the first phase, 28 TBI patients and 28 healthy controls. In the second phase 34 children were studied, 17 TBI patients and 17 controls (27 participants completed both post-acute and chronic phases). We did not find any significant group differences in the post-acute phase. Chronically, we found extensive group differences, mainly for mean and radial diffusivity (MD and RD). In the chronic phase, we found higher MD and RD across a wide range of WM. Additionally, we found correlations between these WM integrity measures and cognitive deficits. This suggests a distributed pattern of WM disruption that continues over the first year following a TBI in children.

1. Introduction

Traumatic brain injury (TBI) is associated with widespread disruptions in white matter (WM) integrity, partly due to traumatic axonal injury (TAI). Intact WM is critical for efficient, healthy brain function, and increasing myelination of WM tracts continues well into the third decade of life (Kochunov et al., 2012) and beyond. WM provides the connections between nodes of distributed neural networks that support higher cognitive processes. Given the long course of WM development and maturation, a TBI during development could potentially delay or alter WM maturation, and subsequently affect the cognitive functions supported by disrupted fiber tracts. Our study attempts to answer some questions about how TBI during development impacts WM integrity, and the extent to which these disruptions are linked with cognitive impairment following TBI.

TAI is linked to a wide range of impairments and is a progressive process, but TAI can only be diagnosed with certainty *post mortem* (Büki and Povlishock, 2006). While traditional computed tomography (CT) and magnetic resonance imaging (MRI) methods can detect TAI, recent studies have suggested the need for diffusion weighted imaging (DWI) as well (Xu et al., 2007; Lee et al., 2008). DWI methods such as high angular resolution diffusion imaging (HARDI) combined with tractography allow us to visualize axonal pathways *in vivo* and assess their microstructural integrity. Fractional anisotropy (FA), the degree to which water diffuses preferentially in one direction (along axons), is the most common measure of WM integrity. Generally, higher FA

* Correspondence to: Keck School of Medicine, University of Southern California, 2001 N. Soto Street, Los Angeles, CA 90033, USA. Tel.: +1 323 442 7246; fax: +1 323 442 0137.
E-mail address: pthomp@usc.edu (P.M. Thompson).

means better myelinated, more highly developed tracts (Thomason and Thompson, 2011), although there are exceptions to this rule (Budde et al., 2011). FA is a scalar value between 0 and 1 that describes the degree to which water is diffusing in a primary direction (anisotropic) versus all directions equally (isotropic), calculated by this equation:

$$FA = \sqrt{\frac{3}{2}} \frac{\sqrt{(\lambda_1 - \hat{\lambda})^2 + (\lambda_2 - \hat{\lambda})^2 + (\lambda_3 - \hat{\lambda})^2}}{\sqrt{\lambda_1^2 + \lambda_2^2 + \lambda_3^2}}$$

To better understand factors that might contribute to differences in FA, we also analyzed various component and related measures: axial diffusivity (AD — a measure of diffusivity along the principal direction of diffusion, λ_1), radial diffusivity (RD — average of the diffusivity along the other two eigenvectors, average of λ_2 and λ_3), and mean diffusivity (MD — average of diffusivity in all directions, also called ADC — apparent diffusion coefficient, $\hat{\lambda}$). A decrease in FA could be caused by a decrease in AD, which may suggest axonal degeneration (although this is a difficult measure to interpret), or it could also be caused by an increase in RD, which would suggest myelin damage (Budde et al., 2011; Mac Donald et al., 2007). Prior studies examining WM integrity following TBI have largely found decreased FA and increased RD, suggesting the latter interpretation (Farbota et al., 2012; Caeyenberghs et al., 2011; Dinkel et al., 2014; Ewing-Cobbs et al., 2008; Oni et al., 2010), two of these studies focused on pediatric patients (Ewing-Cobbs et al., 2008; Oni et al., 2010).

Immediately after TBI, FA tends to increase and ADC (MD) decreases, likely reflecting edema and inflammation (Wilde et al., 2008; Yallampalli et al., 2013; Barzó et al., 1997; Marmarou et al., 2006). In the post-acute (or sub-acute) and chronic phases of TBI, FA decreases, and MD and RD increase (Xu et al., 2007; Farbota et al., 2012; Caeyenberghs et al., 2011; Dinkel et al., 2014; Ewing-Cobbs et al., 2008; Oni et al., 2010; Wozniak et al., 2007; Yuan et al., 2007; Sidaros et al., 2008; Levin et al., 2008; Bendlin et al., 2008; Greenberg et al., 2008; Wu et al., 2010; Caeyenberghs et al., 2010; Pal et al., 2012; Wilde et al., 2012). While there is a considerable amount of heterogeneity across patients, the corpus callosum is the most commonly reported area of disruption (Xu et al., 2007; Farbota et al., 2012; Caeyenberghs et al., 2011; Dinkel et al., 2014; Ewing-Cobbs et al., 2008; Yuan et al., 2007; Sidaros et al., 2008; Levin et al., 2008; Bendlin et al., 2008; Wu et al., 2010; Wilde et al., 2012), with studies reporting widespread decreases in FA and increases in RD and MD in the post-acute and chronic phases of TBI. Studies have also reported disrupted integrity in the internal (Xu et al., 2007; Yuan et al., 2007; Sidaros et al., 2008; Levin et al., 2008; Bendlin et al., 2008; Wilde et al., 2012) and external capsules (Xu et al., 2007; Bendlin et al., 2008), the cingulum bundle (Bendlin et al., 2008; Pal et al., 2012; Wilde et al., 2012), cingulate gyrus (Xu et al., 2007; Wilde et al., 2012), fornix (Xu et al., 2007; Yallampalli et al., 2013; Pal et al., 2012; Wilde et al., 2012), thalamus (Bendlin et al., 2008; Wilde et al., 2012), superior longitudinal fasciculus (Xu et al., 2007; Farbota et al., 2012; Yuan et al., 2007; Bendlin et al., 2008; Pal et al., 2012), inferior fronto-occipital fasciculus (Bendlin et al., 2008; Pal et al., 2012), centrum semiovale (Yuan et al., 2007; Sidaros et al., 2008; Wilde et al., 2012), posterior thalamic radiations (Caeyenberghs et al., 2010; Pal et al., 2012), optic radiations (Farbota et al., 2012; Wu et al., 2010), and cerebral peduncles (Sidaros et al., 2008; Bendlin et al., 2008). Taking a broader view of WM integrity, the frontal (Oni et al., 2010; Wozniak et al., 2007; Levin et al., 2008; Wilde et al., 2012), temporal (Levin et al., 2008; Wilde et al., 2012), parietal (Wilde et al., 2012), and occipital lobes (Wilde et al., 2012) have all been shown to have disrupted WM. Numerous investigations of pediatric patients have shown how TBI during development impacts WM integrity and development (Ewing-Cobbs et al., 2008; Oni et al., 2010; Yallampalli et al., 2013; Wozniak et al., 2007; Yuan et al., 2007;

Levin et al., 2008; Wu et al., 2010; Caeyenberghs et al., 2010; Wilde et al., 2012, 2011). Longitudinal studies are fewer, but are important for determining how TBI impacts development. Wu et al. (2010) assessed 23 moderate/severe TBI participants (msTBI) and 25 with orthopedic injury (OI) between ages 7 and 17 years old at 2 timepoints — 3 months post-injury and 18 months post-injury (Wu et al., 2010). At 3 months, they found lower FA and higher ADC in the whole corpus callosum, as well as the sub-divisions — the genu, body, and splenium. At 18 months, these differences largely persisted. While they found no group differences in processing speed, they did find an association between FA and processing speed at both time points. In another study of an overlapping cohort, Wilde et al. using TBSS found wide areas of lower FA at 3 months, while ADC differences were more prominent at 18 months (Wilde et al., 2012). Longitudinally, the OI group showed increases in FA, as expected with continued maturation, while the moderate/severe (msTBI) group showed FA decreases and ADC increases, indicating continuing degeneration, although there were some areas of ADC decrease. Depending on the type, location, and severity of the injury, pre-existing conditions, home support, and numerous other factors, these measures can be quite heterogeneous across TBI patients.

We examined TBI at two distinct, circumscribed time points post-TBI in a large, pediatric cohort. In this study, we examined pediatric (8–19 years old) msTBI participants in the post-acute phase (1–5 months post-injury) and again in the chronic phase (13–19 months post-injury). We used high angular resolution diffusion imaging (HARDI) for improved resolution of crossing fibers, and a newly developed method for fiber extraction and tractography, auto-MATE (automated multi-atlas tract extraction) (Jin et al., 2012, 2013, 2014). We expected that these advanced methods would enable us to detect more subtle disruptions than are detectable with existing methods. We hypothesized that we would find decreased white matter integrity in the TBI group, especially in the corpus callosum, but in peripheral tracts as well. We hypothesized that disruptions found in the post-acute phase would progress in the chronic phase, and that these disruptions would be related to cognitive deficits. If our hypotheses are correct this method of analyzing DTI data may prove useful as a biomarker of recovery and a target of interventions.

2. Methods

2.1. Participants

TBI participants were recruited from 4 Pediatric Intensive Care Units (PICUs) located in Level 1 Trauma Centers in Los Angeles County. In these institutions, patients with moderate or severe TBI are routinely admitted to the PICU. The Study or Site Coordinator discussed the investigation with the parents of patients, gave them an IRB approved brochure about the study and obtained permission for the investigators to contact them upon discharge. Thirty-five percent of patients whose parents agreed to be contacted while the child was in the PICU participated in this study. Out of 114 families contacted at the PICUs, 27 were lost to contact (kept canceling/rescheduling), 21 did not qualify because they did not meet the criteria (GCS greater than 12, English skills not sufficient, ADHD, learning disability, braces, etc.), 25 were not interested, and 37 are participating and 4 are pending. Healthy controls, matched for age, sex, and educational level, were recruited from the community through flyers, magazines, and school postings. We studied 28 children with moderate to msTBI and 28 healthy control children in the post-acute phase (1–5 months post injury) and evaluated 17 msTBI and 17 healthy control children in the chronic phase (13–19 months post-injury). Several participants were only scanned in the chronic phase, while a few scanned in the post-acute phase were scanned outside the 1–5 month window, and were thus not included in analyses. For those participants who completed the longitudinal assessment, the chronic assessment was completed

Table 1
Demographics. Demographic information on the participants included. Information is listed for both the post-acute phase (1–5 months post-injury), and the chronic phase (13–19 months post-injury). We list the number of TBI and control participants in each phase, the male/female ratio, and the average age of these groups (and standard deviation).

	Phase			
	Post-acute		Chronic	
	TBI	Control	TBI	Control
N	28	28	17	17
M/F	19/9	19/9	12/5	12/5
Age	14.0 (2.7)	14.7 (3.0)	16.0 (2.4)	16.4 (2.9)

approximately 12 months after the post-acute assessment. Demographics of the participants included in cross-sectional analyses of the post-acute and chronic phases are presented in Table 1. The injury mechanisms for our TBI group were as follows: 28% motor vehicle accident (MVA) — pedestrian, 17% skateboard, 14% MVA — passenger, 10% scooter, 7% bike, 7% blunt head trauma from sports, 3% assault, 3% skiing, 3% fall from ladder, 3% uncategorized fall, and 3% uncategorized blunt head trauma.

2.1.1. Inclusion criteria

1) Non-penetrating msTBI (intake or post-resuscitation GCS score between 3 and 12); 2) 8–19 years of age; 3) right-handed; 4) normal visual acuity or vision corrected with contact lenses/eyeglasses; and 5) English skills sufficient to understand instructions and be familiar with common words (the neuropsychological tests used in this study presume competence in English).

2.1.2. Exclusion criteria

1) History of neurological illness, such as prior msTBI, brain tumor or severe seizures; 2) motor deficits that prevent the subject from being examined in an MRI scanner (e.g. spasms); 3) history of psychosis, ADHD, Tourette's Disorder, learning disability, mental retardation, autism or substance abuse. These conditions were identified by parental report and are associated with cognitive impairments that might overlap with those caused by TBI. Participants were excluded if they had metal implants that prevented them from safely undergoing an MRI scan.

2.2. Scan acquisition

Participants were scanned on 3T Siemens Trio MRI scanners with whole brain anatomical and 66-gradient high angular resolution diffusion imaging (HARDI). Diffusion-weighted images (DWI) were acquired with the following acquisition parameters: GRAPPA mode; acceleration factor PE = 2; TR/TE = 9500/87 ms; FOV = 256 × 256 mm; isotropic voxel size = 2 mm. 66 images were collected per subject: 2 b_0 and 64 diffusion-weighted ($b = 1000$ s/mm^2).

2.3. Scan comparison

Part-way through the study, scanning moved from the UCLA Brain Mapping Center (BMC) to the Staglin IMHRO Center for Cognitive Neuroscience (Staglin). Both scanners were 3T Siemens Trio scanners, and the protocol was maintained. To determine that this scanner change did not introduce bias into our data, we scanned 6 healthy adult volunteers at both the BMC and Staglin centers, 1.5 months apart, as well as a DTI phantom, purchased specifically to gauge the impact of the scanner change on standard metrics from DTI. We then assessed possible bias in both the DTI and T1-weighted images. To assess sources of bias in the DTI data, we ran our autoMATE method on the subjects, giving us comparable data on the WM integrity across

the fiber indices. We then ran a 2-tailed paired t-test on these data files for the 6 subjects, and detected no significant effect of scanner.

For the T1-weighted images, we first compared the bias maps using the *nu_estimate* tool from the MINC Tool Kit (http://www.bic.mni.mcgill.ca/ServicesSoftware/ServicesSoftwareMincToolKit). After N3 correction, which is a standard pre-processing step for T1-weighted images to correct for variation in image intensity, we calculated the residual intensity correction field on both the BMC and Staglin files. Our aim here was to determine if there was significant scanner induced bias in the image intensity, which can affect image registration and volume calculations. The comparison revealed no detectable pattern in the difference between the intensity correction fields above noise, except in the cerebellum, where there appeared to be scanner induced differences in image intensity even after N3 correction. Future studies of regional volume in this cohort will exclude the cerebellum for this reason, or limit analyses to subjects scanned at only one scanner.

In addition to the bias maps, we investigated possible differences in computed regional brain volume. To do this, we completed our tenser-based morphometry workflow (Hua et al., 2008), which we have applied to over 4000 scans as part of the ADNI project. Briefly, we N3-corrected and created masks of the files. One subject was selected to be the study specific template, as that has been shown to improve registration. The other 5 subjects were linearly registered to this subject using *flirt* with 6 DOF. Once subjects' scans were co-registered they were masked, using the same subject-specific mask for the BMC and Staglin data to ensure comparability around the edges of the brain. Each subject's BMC scan was non-linearly registered to their Staglin scan (32 FFT × 300 iterations). The inter-subject displacement vector field U_{inter}^n 5 (u_x, u_y, u_z), obtained from this step, was then applied to transform the Jacobian change map of each subject's BMC T1-weighted image to the brain coordinate defined by that subject's Staglin T1-weighted image. In this way, we generated maps of the regional volume difference between T1-weighted images of the two scanners. These Jacobians were averaged across subjects, and the resulting image indicated that, again, there was no pattern above noise indicating a significant effect of scanner, with the exception of the cerebellum.

At this point, we also created a minimal deformation template (MDT) from our volunteer subjects. The MDT is the template that deviates least from the anatomy of the subjects, and, in some circumstances, it can improve statistical power to detect regional brain differences (Leporé et al., 2007). The N 3D vector fields that fluidly registered a specific individual to all other N subjects were averaged and applied to that subject, preserving the image intensities and anatomical features of the template subject. We then non-linearly registered the T1-weighted images from the BMC and Staglin scanners to the MDT in the same manner as above, generating Jacobian maps indicating the regional volume difference between each T1-weighted image and the MDT. These were then entered into a voxel-wise linear regression testing the association between regional volume and age (separately for the BMC and Staglin data), with the simple aim of checking whether the statistical maps differed between BMC and Staglin. Again, the resulting statistical files were similar, indicating that there was no detectable statistical bias introduced by the scanner effect. These tests together give us confidence that the change in scanner did not introduce any additional source of noise or bias. Even so, in our analyses we did include a covariate for scanner in our regression models.

2.4. Cognitive measures

Participants completed a battery of cognitive tests at both time 1 and time 2. Age-based standardized or scaled scores were used from the following measures: the CVLT-C (California Verbal Learning Test, Children's Version) (Delis et al., 1994) or the CVLT-II (California Verbal Learning Test — Second Edition — for participants aged 16 years and older), D-KEFS Verbal Fluency, Color–Word Interference Subtest, Trail

Making Test (Delis et al., 2001), WISC-IV or WAIS-II Processing Speed Index (PSI) (Wechsler, 2003), and WISC-IV or WAIS-III Working Memory Index (WMI) (Wechsler, 2003). The CVLT (child or adult version) Trials 1–5 score assesses verbal learning and short-term memory. The Verbal Fluency (total correct) measure assesses executive functioning and linguistic skills. On the Color–Word subtest, the Stroop-like condition required participants to inhibit overlearned responses by naming colors instead of reading words. Condition 4 of the Trail Making Test was a measure of switching attention. The WISC and WAIS based Processing Speed Index was comprised of the Coding and Symbol Search subtests. For the Working Memory Index, the Digit Span and the Letter–Number Sequencing subtests were included. Of note, however, the WAIS-III WMI requires a third subtest to be administered to derive the Index score; instead, the average of the Digit Span and Letter–Number Sequencing scaled scores were added to the latter to derive WMI only on the WAIS-III.

2.5. Tractography

AutoMATE (automated multi-atlas tract extraction), developed by our laboratory, is described fully in prior papers (Jin et al., 2012, 2013, 2014). The workflow is shown in Fig. 1. HARDI images were corrected for eddy-current induced distortions using the FSL tool "eddy_correct" (http://fsl.fmrib.ox.ac.uk/fsl/). DWI scans were skull-stripped using "BET". FA and MD maps were computed using "dtifit". Whole-brain tractography was performed with Camino (http://cmic.cs.ucl.ac.uk/camino/). The maximum fiber turning angle was set to 35°/voxel to limit biologically implausible results, and tracing stopped when fractional anisotropy (FA) dropped below 0.2, as is the standard in the field.

2.6. Fiber clustering and label fusion

As part of autoMATE, five WM tract atlases were constructed from healthy young adults' (20–30 years old) HARDI data, as detailed further in prior papers (Jin et al., 2012, 2013, 2014). The atlas, based on the "Eve" brain atlas (Zhang et al., 2010a), includes 18 major WM tracts: the anterior thalamic radiation (left and right — atr_l and atr_r), corticospinal tract (left and right — cst_l and cst_r), cingulum (left and right — cgc_l and cgc_r), inferior fronto-occipital fasciculus (left and right — ifo_l and ifo_r), inferior longitudinal fasciculus (left and right — ilf_l and ilf_r), arcuate fasciculus (left only — slf_l, as the right slf is too asymmetric for population studies to be practical (Catani et al., 2007)), fornix, and corpus callosal tracts divided into 6 segments — frontal, precentral gyrus, postcentral gyrus, parietal, temporal, and occipital. The Eve atlas was registered, linearly and then non-linearly,

to each subject's FA map using ANTs (Advanced Normalization Tools (Avants et al., 2011)) and its ROIs were correspondingly warped to extract 18 tracts of interest for each subject based on a look-up table (Zhang et al., 2010b). Each subjects' FA map was further registered non-linearly to each of the 5 manually constructed atlases. Registrations were visually inspected for quality. We refined fiber extractions of each tract based on the distance between the corresponding tract of each atlas and the subject's fiber candidates from ROI extraction. Individual results from the 5 atlases were fused. We visually inspected the resulting fiber bundles. For each of the 18 WM tracts, we selected one example subject to display results of group analyses.

2.7. Fiber tracking

As TBI can lead to decreases in FA, and can cause difficulties in tracking fibers in TBI (Xu et al., 2007), this can lead to an issue with some methods that more severely disrupted areas are skipped in analysis, which could bias results or give researchers an incomplete picture. As with other methods, diffusivity measures are assessed along the fibers, but unlike other methods, our group comparisons are not constrained to where fibers were reconstructed. In an area of low FA, where a fiber might be dropped, the FA at the point in the registered FA map is used for group comparison. Diffusivity measures at the point are interpolated to subvoxel resolution. The fiber maps are used to generate standardized spaces in which to conduct group comparisons, and allow us to state that our results indeed belong to tract A vs. tract B, but the group comparisons do not depend on these fiber tracts. All subjects are compared in the space of one subject's fiber coordinates, after registering each subject's FA map to that example subject's FA.

2.8. Group comparison

To limit our search area, as the fiber data results in >100,000 data points, we averaged FA, MD, RD, and AD within each of the 18 tracts and ran group analyses on those summary measures. FA was our primary measure of interest, and pending significant results in FA, we followed up with *post hoc* analyses of MD, RD and AD to determine what was driving the results. These were corrected for multiple comparisons using the FDR method (false discovery rate) (Benjamini, and Hochberg, 1995) ($q < 0.05$). We then followed up on those tracts where we found significant differences in average diffusivity measures, examining the point-wise data with a point-wise matching scheme across the entire population (Jin et al., 2013, 2014). We ran an element-wise linear regression testing for group differences, including
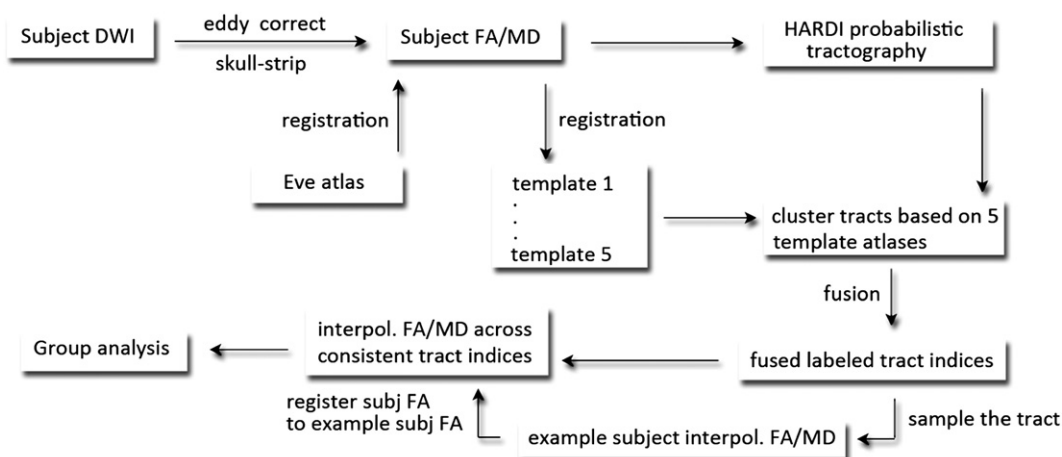

Fig. 1. Workflow. The workflow of autoMATE, described in the methods section and in further detail in Jin et al. (2013) (Jin et al., 2012, 2013, 2014).

age, sex and scanner as covariates. This was run separately for the post-acute and chronic data. Results were corrected for multiple comparisons using FDR across all points on those tracts tested ($q < 0.05$). To be clear, these were not corrected across all 100,000+ data points for FA, and 300,000+ data points for MD/RD/AD; they were just corrected across tracts whose average results merited follow-up.

2.9. Cognitive analyses

Similar to our group analysis, we began our analysis of cognitive correlates of the diffusivity measures by examining the average tract measures. From there, we followed up on the tracts that showed significant differences in average diffusivity to the whole-tract data. For this analysis we ran an element-wise linear regression testing for association between the cognitive measures and the diffusivity measures along the tracts, including age, sex, scanner, and group as covariates. TBI and control subjects were run together, but all results were followed up in each group separately as well. Results were corrected for multiple comparisons using FDR across all points on all tracts tested across all cognitive measures tested ($q < 0.05$). Again FA was our primary diffusivity measure of interest, and MD, RD, and AD were analyzed *post hoc*. We also tested whether GCS upon hospital admission was associated with WM integrity (Glasgow Coma Scale (Teasdale et al., 1979)).

To check for possible cohort effects, we tested for significant differences between the TBI patients included in the post-acute phase and chronic phase. They did not differ significantly in sex distribution ($p = 0.85$), severity, as measured by GCS upon hospital admission ($p = 0.76$), or focal lesions ($p > 0.05$ for contusions, subdural hematoma, subarachnoid hemorrhage, intracerebral hematoma, or epidural hematoma).

3. Results

3.1. Post-acute

When examining averaged FA, MD, RD, and AD across all 18 tracts, we found significantly lower average FA in the TBI group in the ifo_l and ilf_l (crit. FDR threshold = 0.0043, Table 2). Upon follow-up of the tracts element-wise, there were no significant differences that survived correction for multiple comparisons. We did not find any differences in our *post hoc* analyses of RD, MD, or AD in the initial tract average analysis. We also tested whether the time since injury (number of weeks between injury and time 1 assessment) was associated with any measure of WM integrity. We detected no significant associations between time since injury and WM integrity.

3.2. Chronic

In the chronic phase, we again started with tract averages, finding differences in average FA in a number of tracts, as well as our *post hoc* analyses of RD, MD, and AD. For average FA, we found lower average FA in TBI in the cc_frontal, cc_temporal, cgc_l, cgc_r, cst_r, ifo_r, and ilf_r (crit. FDR threshold = 0.0175). We found greater average RD in TBI in the cc_frontal, cc_parietal, cc_temporal, cc_occipital, cc_prcg, atr_l, atr_r, cgc_l, cgc_r, cst_r, ifo_r, ilf_l, ilf_r, and fornix (crit. FDR threshold = 0.032). Similarly, we found greater average MD in TBI in all of the tracts listed above, as well as the cc_pocg and cst_l (corrected for multiple comparisons along with RD and AD). For AD, we found greater average AD in TBI in the cc_occipital, atr_l, atr_r, ifo_r, ilf_l, ilf_r, and fornix (corrected for multiple comparisons along with RD and MD). Average diffusivity measures, as well as standard deviation and Cohen's *d* for both groups across tracts showing significant group differences are shown in Table 2 and Table 3.

We then followed up on these measures in these tracts element-wise. We found much more extensive differences in the chronic phase than the post-acute phase generally. RD and MD differences were much more pronounced than differences in AD, with only a few tracts showing significant differences in AD in limited areas. There were no significant differences in FA element-wise. As nearly all of the tracts showed RD and MD effects, we will break down our discussion of these results into the commissural, association, and projection tracts. These results are shown in Table 4.

We also tested whether time since injury (number of weeks between injury and time 2 assessment) was associated with any measure of WM integrity. There were no significant associations detected between time since injury and WM integrity.

3.2.1. Commissural tracts

In the CC_frontal segment, we saw extensive regions of greater MD and RD in TBI specifically in the lateral projections of the body and genu, rather than the body itself (Fig. 2). In the CC_prcg segment, we found greater MD and RD in TBI again in the lateral projections from the body. Similarly in the CC_pocg segment, we found greater MD in TBI in the lateral projections. In the CC_parietal this pattern held, with greater MD and RD in TBI in the lateral projections. In the CC_temporal segment, we found greater MD and RD in the projections of the *splenium*; results appeared more pronounced in the right hemisphere. In the CC_occipital segment, we found greater MD and RD in the projections of the splenium, and the *forceps major*. These results can be seen in Fig. 3.

3.2.2. Association tracts

The TBI group had greater MD and RD along the cingulum, bilaterally (cgc_l and cgc_r), with the most pronounced results in the parietal aspect. In the ifo_r, we found greater RD and MD along the ifo_r, with the most pronounced results in the posterior, parietal aspect of the tract. In the ilf_l, the TBI group had greater MD in the anterior aspect of the tract, as well as a cluster running along the inferior aspect of the tract. In the ilf_r, the TBI group had small, scattered regions of greater

Table 2

Tract average results — postacute. The results of the group analysis of the tract averages, corrected for multiple comparisons, within measure, using FDR ($q < 0.05$). Diffusivity measures were averaged within tracts, these were used as a starting point for the analysis to contain the search space. Group averages (and SD in parentheses) are shown for FA, MD, RD, and AD across the 18 tracts tested; those that survived FDR are presented in bold-face. Cohen's *d* is also reported for those showing a significant group difference. Tracts whose average diffusivity measures were significantly different between groups were followed up for whole-tract analyses.

	Postacute		
	FA		
	Control	TBI	Cohen's *d*
CC_frontal	5.94E−01 (3.84E−02)	5.69E−01 (3.10E−02)	−
CC_prcg	5.88E−01 (4.45E−02)	5.80E−01 (3.72E−02)	−
CC_pocg	5.57E−01 (4.86E−02)	5.48E−01 (4.24E−02)	−
CC_parietal	5.79E−01 (4.29E−02)	5.72E−01 (3.60E−02)	−
CC_temporal	6.55E−01 (6.01E−02)	6.42E−01 (3.26E−02)	−
CC_occipital	6.68E−01 (6.42E−02)	6.49E−01 (5.53E−02)	−
Atr_l	4.71E−01 (2.59E−02)	4.53E−01 (4.42E−02)	−
Atr_r	4.87E−01 (3.03E−02)	4.71E−01 (4.27E−02)	−
Cgc_l	4.87E−01 (3.53E−02)	4.75E−01 (4.01E−02)	−
Cgc_r	4.63E−01 (3.58E−02)	4.45E−01 (5.45E−02)	−
Cst_l	5.72E−01 (2.63E−02)	5.62E−01 (3.27E−02)	−
Cst_r	5.86E−01 (4.82E−02)	5.79E−01 (4.00E−02)	−
Ifo_l	**5.16E−01 (3.27E−02)**	**4.84E−01 (3.86E−02)**	0.89
Ifo_r	5.09E−01 (4.29E−02)	4.86E−01 (4.74E−02)	−
Ilf_l	**5.37E−01 (3.57E−02)**	**5.00E−01 (4.30E−02)**	0.94
Ilf_r	5.13E−01 (5.04E−02)	4.83E−01 (4.56E−02)	−
Slf_l	4.84E−01 (3.38E−02)	4.68E−01 (4.31E−02)	−
Fornix	3.85E−01 (4.51E−02)	3.56E−01 (6.13E−02)	−

Table 3

Tract average results — chronic. The results of the group analysis of the tract averages, corrected for multiple comparisons, within measure, using FDR ($q < 0.05$). Diffusivity measures were averaged within tracts, these were used as a starting point for the analysis to contain the search space. Group averages (and SD in parentheses) are shown for FA, MD, RD, and AD across the 18 tracts tested; those that survived FDR are presented in boldface. Cohen's d is also reported for those showing a significant group difference. Tracts whose average diffusivity measures were significantly different between groups were followed up for whole-tract analyses.

| | Chronic | | | | | | | | | | | |
| | FA | | | MD | | | RD | | | AD | | |
	Control	TBI	Cohen's d	Control	TBI	Cohen's d	Control	TBI	Cohen's d	Control	TBI	Cohen's d
CC_frontal	**5.96E−01** **(1.92E−02)**	**5.59E−01** **(3.15E−02)**	1.42	**7.35E−04** **(1.68E−05)**	**7.75E−04** **(2.92E−05)**	−1.68	**4.60E−04** **(1.98E−05)**	**5.13E−04** **(4.12E−05)**	−1.63	1.27E−03 (2.89E−05)	1.28E−03 (3.45E−05)	—
CC_prcg	5.90E−01 (2.54E−02)	5.56E−01 (4.86E−02)	—	**7.88E−04** **(2.29E−05)**	**8.20E−04** **(3.04E−05)**	−1.20	**5.11E−04** **(2.71E−05)**	**5.55E−04** **(5.50E−05)**	−1.03	1.35E−03 (4.78E−05)	1.35E−03 (5.96E−05)	—
CC_pocg	5.53E−01 (3.46E−02)	5.23E−01 (5.44E−02)	—	**8.26E−04** **(3.97E−05)**	**8.52E−04** **(4.65E−05)**	−0.61	5.61E−04 (4.82E−05)	5.97E−04 (6.58E−05)	—	1.37E−03 (5.57E−05)	1.36E−03 (8.04E−05)	—
CC_parietal	5.84E−01 (2.35E−02)	5.54E−01 (4.46E−02)	—	**7.79E−04** **(2.12E−05)**	**8.08E−04** **(3.75E−05)**	−0.95	**4.95E−04** **(2.72E−05)**	**5.36E−04** **(4.99E−05)**	−1.03	1.34E−03 (4.03E−05)	1.33E−03 (6.58E−05)	—
CC_temporal	**6.79E−01** **(2.20E−02)**	**6.41E−01** **(4.80E−02)**	1.02	**8.41E−04** **(5.42E−05)**	**8.99E−04** **(8.75E−05)**	−0.79	**4.89E−04** **(4.58E−05)**	**5.58E−04** **(9.79E−05)**	−0.89	1.56E−03 (8.33E−05)	1.59E−03 (8.51E−05)	—
CC_occipital	6.72E−01 (3.44E−02)	6.55E−01 (5.44E−02)	—	**7.55E−04** **(1.70E−05)**	**7.91E−04** **(5.07E−05)**	−0.95	**4.26E−04** **(2.73E−05)**	**4.65E−04** **(6.96E−05)**	−0.73	**1.41E−03** **(4.53E−05)**	**1.44E−03** **(4.76E−05)**	−0.67
Atr_l	4.70E−01 (1.73E−02)	4.62E−01 (2.29E−02)	—	**6.98E−04** **(1.28E−05)**	**7.26E−04** **(2.40E−05)**	−1.47	**5.06E−04** **(1.35E−05)**	**5.33E−04** **(2.86E−05)**	−1.19	**1.06E−03** **(1.80E−05)**	**1.09E−03** **(2.23E−05)**	−1.18
Atr_r	**4.95E−01** **(1.84E−02)**	**4.79E−01** **(2.53E−02)**	0.72	**6.83E−04** **(1.40E−05)**	**7.02E−04** **(2.92E−05)**	−0.85	**4.84E−04** **(1.77E−05)**	**5.08E−04** **(3.26E−05)**	−0.91	**1.05E−03** **(2.38E−05)**	**1.08E−03** **(2.15E−05)**	−1.03
Cgc_l	**4.94E−01** **(3.07E−02)**	**4.67E−01** **(3.02E−02)**	0.89	**7.07E−04** **(2.14E−05)**	**7.45E−04** **(2.96E−05)**	−1.46	**5.04E−04** **(2.97E−05)**	**5.44E−04** **(3.49E−05)**	−1.22	1.06E−03 (3.59E−05)	1.08E−03 (3.81E−05)	—
Cgc_r	**4.80E−01** **(2.78E−02)**	**4.45E−01** **(3.00E−02)**	1.21	**6.89E−04** **(2.55E−05)**	**7.15E−04** **(2.89E−05)**	−0.97	**4.97E−04** **(3.00E−05)**	**5.36E−04** **(3.16E−05)**	−1.27	1.01E−03 (3.89E−05)	1.02E−03 (4.63E−05)	—
Cst_l	5.67E−01 (1.85E−02)	5.58E−01 (2.47E−02)	—	**7.07E−04** **(1.39E−05)**	**7.24E−04** **(2.35E−05)**	−0.86	4.68E−04 (1.89E−05)	4.84E−04 (2.82E−05)	—	1.20E−03 (3.02E−05)	1.22E−03 (3.08E−05)	—
Cst_r	**5.95E−01** **(1.91E−02)**	**5.75E−01** **(2.54E−02)**	0.89	**6.81E−04** **(1.89E−05)**	**7.01E−04** **(2.45E−05)**	−0.90	**4.30E−04** **(2.43E−05)**	**4.56E−04** **(2.69E−05)**	−1.04	1.19E−03 (2.45E−05)	1.20E−03 (3.60E−05)	—
Ifo_l	5.16E−01 (2.01E−02)	4.84E−01 (5.24E−02)	—	7.76E−04 (1.55E−05)	8.35E−04 (9.83E−05)	—	5.39E−04 (1.88E−05)	6.09E−04 (1.19E−04)	—	1.20E−03 (3.07E−05)	1.26E−03 (8.03E−05)	—
Ifo_r	**5.22E−01** **(1.68E−02)**	**4.96E−01** **(2.36E−02)**	1.27	**7.55E−04** **(1.88E−05)**	**7.96E−04** **(3.17E−05)**	−1.56	**5.24E−04** **(1.64E−05)**	**5.68E−04** **(3.40E−05)**	−1.64	1.20E−03 (3.50E−05)	1.23E−03 (4.31E−05)	—
Ilf_l	5.36E−01 (1.99E−02)	5.03E−01 (5.34E−02)	—	**7.68E−04** **(1.58E−05)**	**8.27E−04** **(5.75E−05)**	−1.40	**5.25E−04** **(1.23E−05)**	**5.89E−04** **(7.90E−05)**	−1.13	**1.22E−03** **(4.34E−05)**	**1.28E−03** **(6.00E−05)**	−1.23
Ilf_r	**5.22E−01** **(2.10E−02)**	**5.00E−01** **(2.84E−02)**	0.88	**7.61E−04** **(2.02E−05)**	**8.01E−04** **(3.72E−05)**	−1.33	**5.25E−04** **(1.83E−05)**	**5.66E−04** **(3.85E−05)**	−1.36	1.20E−03 (4.17E−05)	1.24E−03 (5.39E−05)	—
Slf_l	4.86E−01 (2.89E−02)	4.66E−01 (5.71E−02)	—	7.11E−04 (1.72E−05)	7.62E−04 (8.07E−05)	—	5.20E−04 (2.82E−05)	5.68E−04 (9.50E−05)	—	1.07E−03 (2.30E−05)	1.13E−03 (6.09E−05)	—
Fornix	3.81E−01 (4.99E−02)	3.33E−01 (7.57E−02)	—	**1.31E−03** **(2.26E−04)**	**1.57E−03** **(3.65E−04)**	−0.86	**1.07E−03** **(2.38E−04)**	**1.35E−03** **(3.87E−04)**	−0.85	**1.78E−03** **(1.95E−04)**	**2.02E−03** **(3.02E−04)**	−0.92

Table 4

Chronic whole-tract results. Whole-tract differences in WM integrity between TBI and control in the chronic phase. For each tract investigated, the FDR threshold is given (we corrected across all points on all tracts tested within diffusivity measure), the minimum p-value for group differences on each tract, and the percentage of the tract that passed the FDR threshold and thus represents areas of significant differences between TBI and control.

| | FA | | | MD | | | RD | | | AD | | |
Cluster	% tract sig.	min. p	FDR thresh.	% tract sig.	min. p	FDR thresh.	% tract sig.	min. p	FDR thresh.	% tract sig.	min. p	FDR thresh.
CC_frontal	—	—	—	4.8	1.1×10^{-7}	0.0019	6.0	1.3×10^{-8}	0.0019	—	—	—
CC_prcg	—	—	—	1.7	3.5×10^{-5}	0.0019	1.1	7.3×10^{-5}	0.0019	—	—	—
CC_pocg	—	—	—	3.9	1.8×10^{-6}	0.0019	—	—	—	—	—	—
CC_parietal	—	—	—	6.3	9.0×10^{-8}	0.0019	3.0	3.8×10^{-6}	0.0019	—	—	—
CC_temporal	—	—	—	2.0	1.1×10^{-5}	0.0019	3.5	1.7×10^{-6}	0.0019	—	—	—
CC_occipital	—	—	—	5.4	1.8×10^{-5}	0.0019	1.4	5.2×10^{-6}	0.0019	0.83	4.6×10^{-7}	0.0019
Atr_l	—	—	—	7.3	4.9×10^{-7}	0.0019	5.4	3.3×10^{-7}	0.0019	1.9	8.8×10^{-7}	0.0019
Atr_r	—	—	—	3.0	1.4×10^{-5}	0.0019	4.4	3.5×10^{-6}	0.0019	0.08	8.5×10^{-5}	0.0019
Cgc_l	—	—	—	5.8	1.1×10^{-5}	0.0019	2.9	2.0×10^{-5}	0.0019	—	—	—
Cgc_r	—	—	—	3.1	1.6×10^{-5}	0.0019	4.6	4.3×10^{-6}	0.0019	—	—	—
Cst_l	—	—	—	0.33	9.7×10^{-5}	0.0019	—	—	—	—	—	—
Cst_r	—	—	—	0.99	7.8×10^{-5}	0.0019	1.6	7.1×10^{-5}	0.0019	—	—	—
Ifo_l	—	—	—	—	—	—	—	—	—	—	—	—
Ifo_r	—	—	—	6.0	7.9×10^{-7}	0.0019	4.3	3.7×10^{-6}	0.0019	—	—	—
Ilf_l	—	—	—	12.0	1.9×10^{-7}	0.0019	4.6	1.2×10^{-6}	0.0019	1.8	0.00017	0.0019
Ilf_r	—	—	—	2.5	1.7×10^{-5}	0.0019	3.8	7.9×10^{-6}	0.0019	—	—	—
Slf_l	—	—	—	—	—	—	—	—	—	—	—	—
Fornix	—	—	—	0.038	0.0016	0.0019	0.08	0.0011	0.0019	0.19	0.0012	0.0019
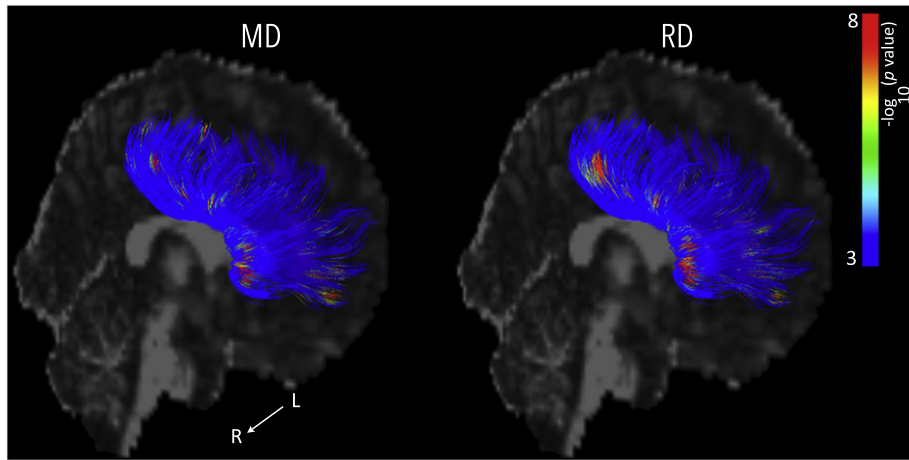
Fig. 2. Chronic results — frontal callosal segment. Whole-tract differences in MD, and RD between TBI and control in the chronic phase in the frontal callosal segment. We found higher MD and higher RD in TBI in these tracts. The −log10 p-values are shown corresponding to the color bar, results were FDR corrected across all points on all tracts tested (those for whom average results indicated follow-up) ($q < 0.05$ MD/RD crit. p threshold = 0.0019).

MD along the main body of the tract, with similar areas of greater RD. These results are shown in Fig. 4. Differences in the fornix were minimal after correction, and thus are not pictured.

3.2.3. Projection tracts

The projection tracts investigated here were the corticospinal tract (cst) and anterior thalamic radiation (atr). In the atr, the TBI group had greater MD and RD in the anterior end of the left and right atr, in the area of the anterior *corona radiata*. There were also small areas of higher MD and RD in the cst_l and cst_r. These results can be seen in Fig. 5.

3.3. Relationships to cognitive performance

The initial analysis of diffusivity tract averages revealed no associations between post-acute cognitive scores and post-acute WM measures. We did find significant associations between chronic cognitive scores and chronic WM measures (Table 5). In the element-wise analysis including all participants, the FDR crit. value for FA was 0.0016, and for MD, RD, and AD it was 0.0067. Again, these were corrected across all points on all tracts whose average results merited follow-up. For all of these, higher FA, lower MD, lower RD,
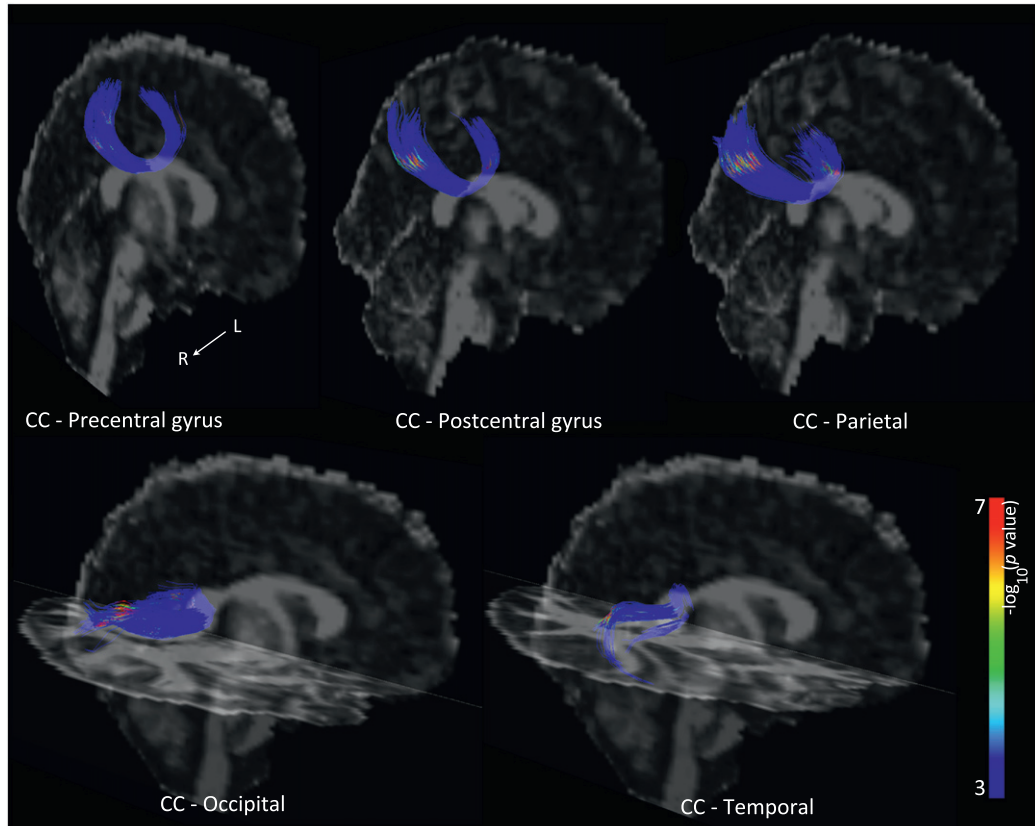
Fig. 3. Chronic results – other callosal segments. Whole-tract differences in MD between TBI and control in the chronic phase in the other callosal segments. We found higher MD and higher RD in TBI in these tracts. RD results had similar localization to the MD results shown here. The −log10 p-values are shown corresponding to the color bar, results were FDR corrected across all points on all tracts tested (those for whom average results indicated follow-up) ($q < 0.05$, MD/RD crit. p threshold = 0.0019).
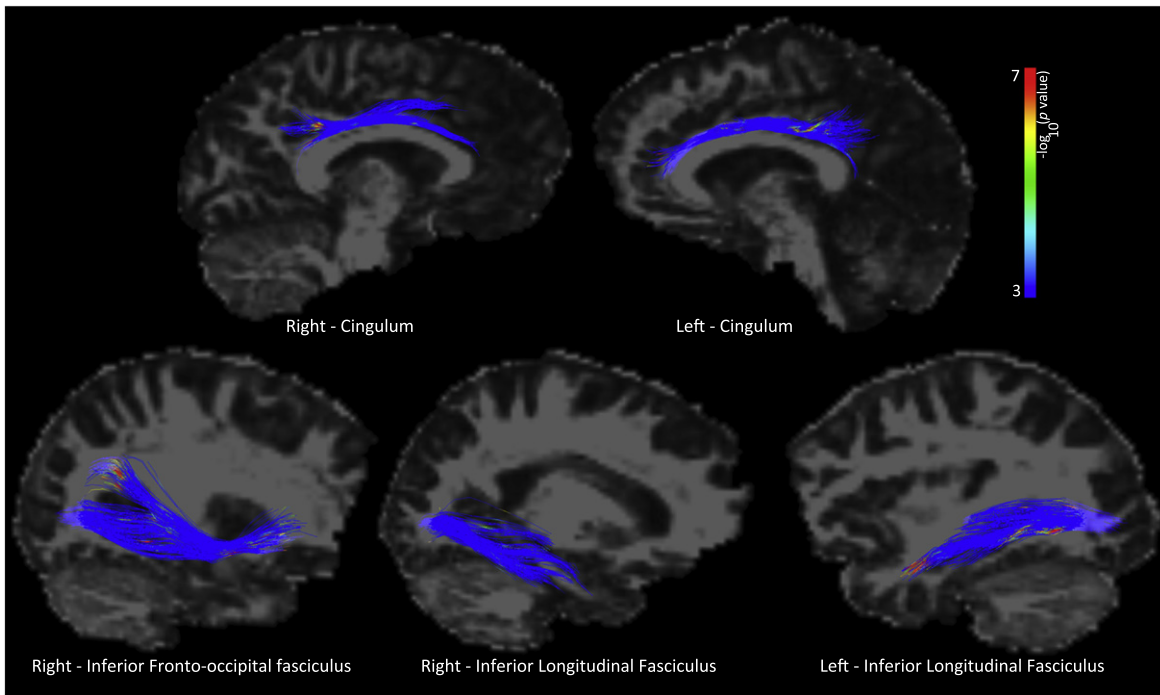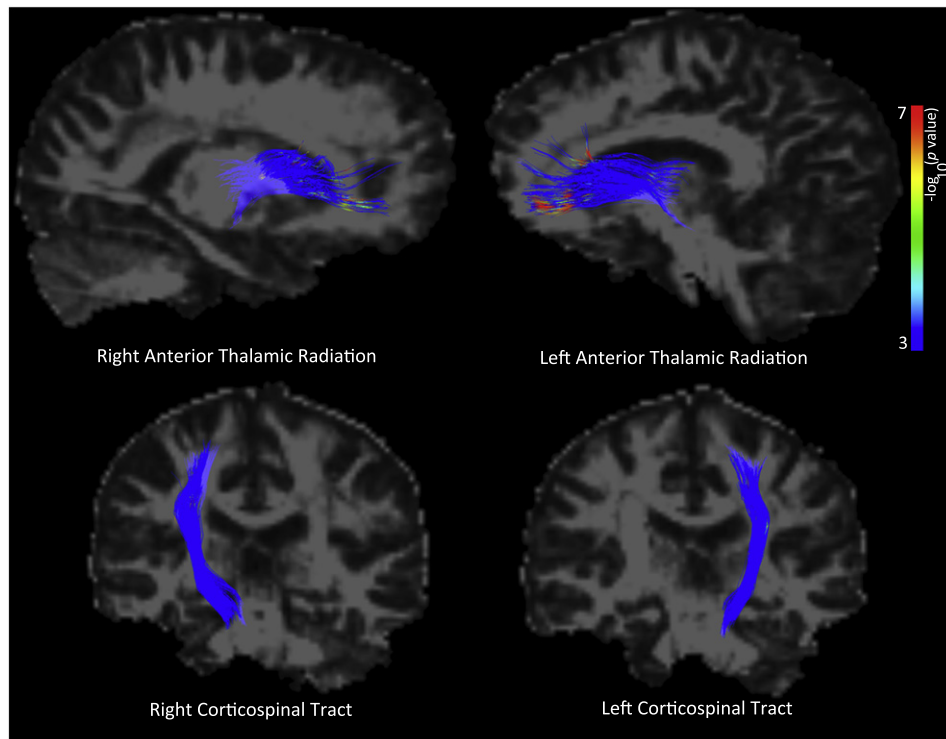
Fig. 4. Chronic results – association tracts. Whole-tract differences in MD between TBI and control in the chronic phase in association tracts. We found higher MD in TBI in these tracts, as well as higher RD in similar areas. The −log10 *p*-values are shown corresponding to the color bar, results were FDR corrected across all points on all tracts tested (those for whom average results indicated follow-up) (*q* < 0.05, MD crit. *p* threshold = 0.0019).

and/or lower AD were associated with better cognitive performance. We found significant associations between CVLT performance and FA of the cst_r. For the inhibition task, we found significant associations between MD, RD, and AD in the ifo_l, as well as MD and RD in the ilf_l. We found associations between processing speed and FA in the ifo_l,

cc_frontal, and cc_parietal, as well as the FA, MD, and RD of the cc_prcg. For the working memory task, we found significant associations between performance and FA in the ifo_l, slf_l, and cc_parietal. Lastly, for the Trails task, we found significant associations between FA, MD, and RD in the cc_frontal, FA and RD in the cc_parietal and

Fig. 5. Chronic results – projection tracts. Whole-tract differences in MD between TBI and control in the chronic phase in projection tracts. We found higher MD in TBI in these tracts, as well as higher RD in similar areas. The −log10 *p*-values are shown corresponding to the color bar, results were FDR corrected across all points on all tracts tested (those for whom average results indicated follow-up) (*q* < 0.05, MD crit. *p* threshold = 0.0019).

Table 5
Cognitive results. Summary table displaying which tracts, diffusivity measures, and cognitive measures we found significant associations between. These are displayed in further detail in Fig. 6 and Fig. 7. All associations were in the direction of better cognitive performance linked with better WM integrity.

	All participants				
	CVLT	Inhibition	PSI	Trails	WMI
Cst_r	FA	—	—	—	—
Ifo_l	—	FA, MD, RD, AD	FA	—	FA
Ilf_l	—	MD, RD	—	—	—
Slf_l	—	—	—	—	FA
CC_frontal	—	—	FA	FA, MD, RD	—
CC_prcg	—	—	FA, MD, RD	—	—
CC_parietal	—	—	FA	FA, RD	FA
CC_temporal	—	—	—	FA, RD	—
CC_occipital	—	—	—	RD	—

cc_temporal, and RD in the cc_occipital. These can be seen in Fig. 6. When we followed up on these results in each group individually, there were no significant results in either group, although there were trend-level associations between inhibition and FA, MD, RD, and AD, in the ifo_l and MD and RD in the ilf_l in the TBI group (Fig. 7). Similarly thresholded maps for the control participants are shown for comparison. GCS was not significantly associated with tract averages post-acutely or chronically, so it was not followed up for whole-tract analyses.

4. Discussion

In this study we used advanced tract analyses to assess WM disruption at two time points during the first year following TBI in pediatric patients. Although TBI is a heterogeneous disorder, WM damage is a hallmark found in the vast majority of cases (Hulkower et al., 2013). The diffuse WM damage in TBI can complicate advanced analyses such as tractography, as FA "dropouts" can lead to premature tract endings (Xu et al., 2007). Here we present an application of a novel method that allows us to assess WM integrity along tracts more robustly and accurately. At the 12-month follow-up, we found significant group differences in WM integrity between TBI and control participants across the majority of tracts tested, however differences in the chronic phase were largely in RD and MD, analyzed *post hoc*. We found no group differences in the post-acute phase that survived correction.

The corpus callosum is one of the commonly reported and replicated areas of WM disruption. Several other studies report lower FA in the corpus callosum in pediatric TBI in the post-acute phase (Levin et al., 2008; Wu et al., 2010; Wilde et al., 2012), and in adult TBI participants in the post-acute phase (Farbota et al., 2012; Sidaros et al., 2008; Pal et al., 2012). As the major commissural tract, the corpus callosum is integral for coordinating activity across hemispheres. Thus, it is unsurprising that researchers have been able to link these characteristic decreases in WM integrity of the corpus callosum in TBI to difficulty with bimanual tasks (Caeyenberghs et al., 2011). Disruption in WM following TBI occurs well beyond the corpus callosum, of course. Decreased FA in the IFOF has also been previously reported in post-acute TBI, in pediatric samples (Wilde et al., 2011), and in adult samples (Farbota et al., 2012; Pal et al., 2012). The IFOF links the frontal and occipital cortices, and while the exact functions of the IFOF remain somewhat mysterious, it appears to play an important role in reading, visual processing, and spatial attention (Catani, and de Schotten, 2012). Decreased FA in the ILF in TBI has been found in adults (Farbota et al., 2012; Pal et al., 2012) and pediatric samples (Levin et al., 2008), and has been linked with decreased performance on the digit symbol substitution test (Pal et al., 2012). Connecting the occipital lobe to the temporal lobes as well as the amygdala and hippocampus, the ILF is critical for language functions, visual memory, face and object perception, and reading (Catani and de Schotten, 2012).

We cannot interpret the null result in the post-acute phase as implying that there are no differences, we are just not able to detect them with the current sample size and methods. We hypothesize that our lack of findings in the post-acute phase is due to regional heterogeneity in the TBI group in regard to where their white matter integrity is impacted. In the post-acute phase, disruption is greatest close to the specific area of injury, but over the first year post injury, this disruption may spread and become global. This may have made group differences easier to detect in the chronic phase. The absence of significant, detectable group differences in the post-acute phase and significant differences in the chronic phase suggests on-going divergence between the groups during the first year post-TBI. This could happen for a number of reasons. The healthy controls are still developing, so we expect their FA to increase with age, as it does appear in our data. Increasing divergence between the groups could also be due to the TBI participants having continual degeneration, or simply displaying slowed or plateauing maturation, as a result of their injury. The lower WM integrity in TBI could be due to Wallerian degeneration, but it could also reflect a slower rate of myelin development. It is likely that there are some TBI patients who experience WM recovery, while others experience continued degeneration; an interesting question for future analyses. Our analyses were cross-sectional, so any interpretation of change over time needs to be replicated by longitudinal analyses. A large portion of these participants included in the post-acute time point have not yet returned for their 12 month assessment, but this study is on-going and future investigations will include more formal longitudinal analyses using a more complete dataset.

In the chronic phase we found extensive group differences in two of the measures analyzed *post hoc*, mean and radial diffusivity (MD and RD), with limited results in axial diffusivity (AD) as well. Prior studies have also found on-going WM degeneration over the first year post-injury, even when cognitive function begins to recover (Bendlin et al., 2008). These changes continue over multiple years post-injury (Farbota et al., 2012), although some studies have found little difference between 2 and 5 years post-injury (Dinkel et al., 2014). All of the corpus callosum (CC) segments showed group differences, with the TBI group having greater MD and RD. These results were consistently localized in the lateral projections of the CC body, genu, and splenium, rather than along the midline. Decreased WM integrity in the CC in the chronic phase is one of the most consistent findings in TBI research (Xu et al., 2007; Farbota et al., 2012; Caeyenberghs et al., 2011; Dinkel et al., 2014; Ewing-Cobbs et al., 2008; Yuan et al., 2007; Sidaros et al., 2008; Bendlin et al., 2008; Wu et al., 2010; Wilde et al., 2012, 2006), although some have failed to find differences (Wozniak et al., 2007). In the anterior thalamic radiation (ATR) we found greater MD and RD in TBI in the anterior projections of the ATR, corresponding to where these tracts terminate in the anterior corona radiata. Other studies have found mixed results in the ATR, with some showing continued deficits while others show evidence of recovery (Farbota et al., 2012; Bendlin et al., 2008). The ATR connects the thalamic nuclei to the orbitofrontal and anterior cingulate cortex (Catani and de Schotten, 2012), thus playing a role in processing sensory information. We also found extensive group differences in association tracts. In the cingulum, we found greater MD and RD in TBI bilaterally in the parietal projections. Decreased WM integrity in the cingulum has been reported previously in chronic TBI participants, both in pediatric samples (Wilde et al., 2012) and in adult samples (Xu et al., 2007; Bendlin et al., 2008). The cingulum follows the shape of the corpus callosum, with short projections branching off to connect the medial frontal cortex, amygdala, parahippocampal gyrus, precuneus, cuneus, cingulate, and fusiform gyri (Catani, and de Schotten, 2012). The cingulum is a key structure in the limbic system, making it integral in emotion, memory, and motivation. In the ILF, we found greater MD and RD in TBI bilaterally, with differences in the anterior-temporal terminus and inferior aspects of the tract in the left hemisphere and more restricted differences in the right hemisphere. The TBI group had greater MD and RD along the
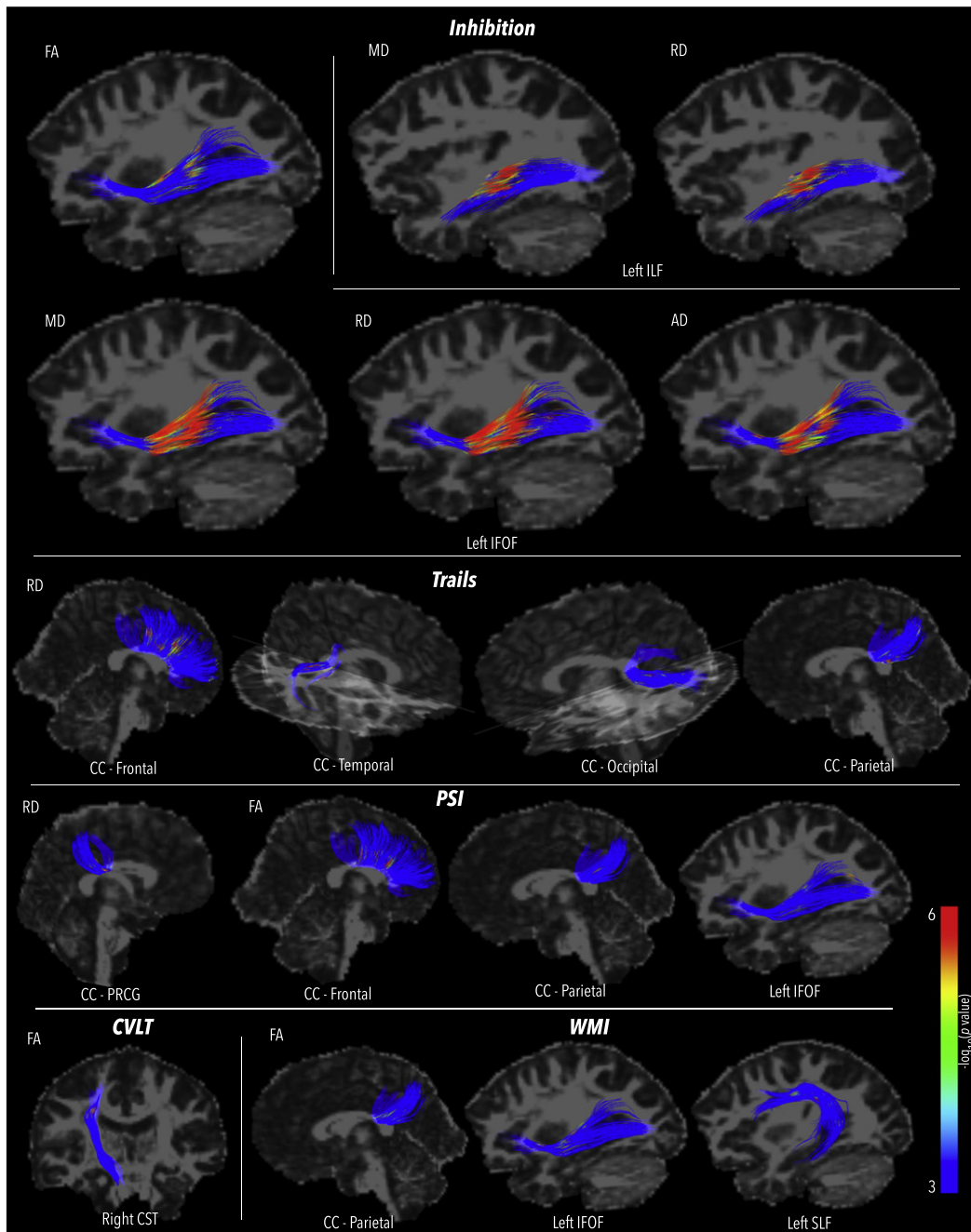
Fig. 6. Cognitive associations across all participants. Whole-tract associations between along-tract FA, MD, RD, and AD and cognitive performance in all participants. All of these were positive correlations between WM integrity and better performance on the cognitive tasks. The −log10 p-values are shown corresponding to the color bar, results were FDR corrected across all points on all tracts tested (those for whom average results indicated follow-up) ($q < 0.05$, FA crit. p threshold = 0.0016, MD/RD/AD crit. p threshold = 0.0067).

tract in the right IFOF, with a particular concentration of differences in the superior parietal projections of the IFOF. Yuan et al. (2007) found a positive relationship between the FA of the IFOF and GCS (Yuan et al., 2007). The anatomy and function of the ILF and IFOF are detailed in the previous paragraph.

While MD and RD results were predominant in the chronic phase, we also found some significant group differences in AD. These were restricted in their anatomical extent, and in the opposite direction to what we might expect: generally we expect FA and AD to increase together with MD and RD decreasing. However, other researchers have reported increases in MD and AD together in TBI (Kinnunen et al., 2010), and increased AD among TBI patients has been associated with improved clinical outcome (Sidaros et al., 2008). These results may

reflect axonal recovery following TBI. Future longitudinal investigations will clarify this.

In this study we assessed participants' cognitive function with 6 different measures, and we found multiple significant associations between these scores on cognitive tests and WM tract integrity. All of these associations were found in the chronic phase. Better processing speed was associated with higher FA and lower MD and RD in the CCs — precentral segment, as well as the FA of the CCs — frontal and CC — parietal segments, and the left IFOF across all participants. Previous studies have linked processing speed to WM integrity of the corpus callosum, fornix, bilateral ILF and bilateral IFOF (Yallampalli et al., 2013; Wu et al., 2010; Marquez de la Plata et al., 2011). Better performance on the inhibition task, a test of cognitive flexibility and the ability
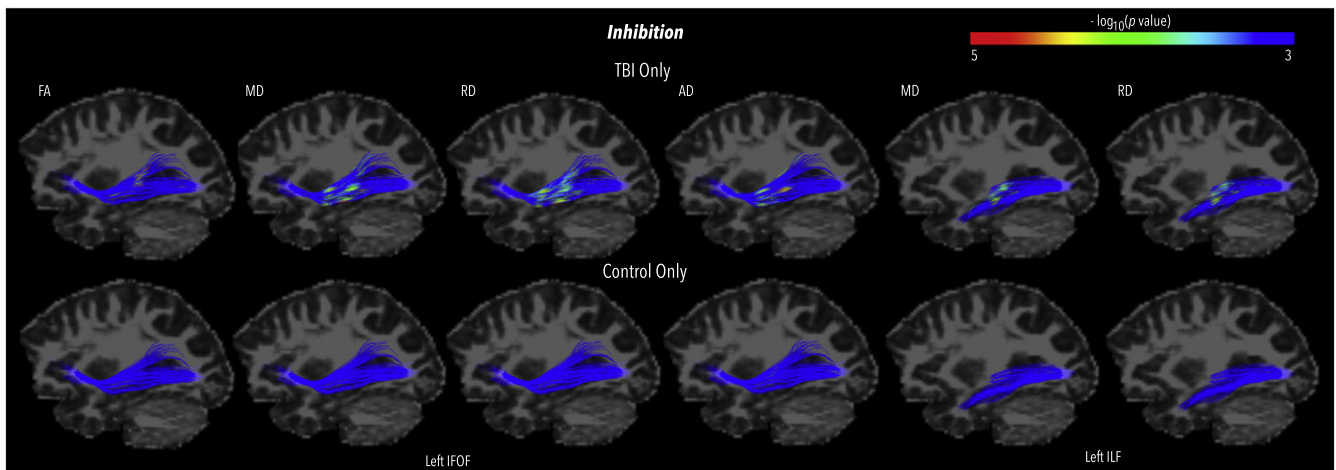
Fig. 7. Cognitive associations in TBI and control participants. Whole-tract associations between WM integrity in the left IFOF and ILF and performance on the inhibition task. These were positive correlations between WM integrity and better performance on the task. The −log10 p-values are shown corresponding to the color bar, results did not pass FDR across all tracts tested, these are trend-level associations demonstrating the relative contributions of the TBI and control groups. The crit. p thresholds from the all-subject analyses were used to threshold these images (FA = 0.0016, MD/RD/AD = 0.0067).

to inhibit conflicting information, was broadly associated with higher FA and lower MD, RD, and AD of the left IFOF as well as lower MD and RD of the left ILF, across all participants and at a trend level in just the TBI participants, which overlaps with findings from earlier studies (Marquez de la Plata et al., 2011). These results suggest that among individuals who have sustained TBI, deficits in WM integrity in the left IFOF and ILF are linked with poorer performance on the inhibition task. When we have more participants at this time point, we can further investigate group contributions to the cognitive associations. Better performance on the trails task, indicative of mental flexibility and efficient processing, was associated with higher FA, lower MD and RD in the CCs — frontal segment, higher FA and lower RD in the parietal and temporal segments, and lower RD in the CCs — occipital segment across all participants, also overlapping with prior findings (Marquez de la Plata et al., 2011). Better working memory performance was associated with higher FA in the CCs — parietal segment, left IFOF, and the left SLF. Prior studies on working memory in TBI have implicated the splenium, cingulum, and frontal lobe (Ewing-Cobbs et al., 2008; Wilde et al., 2011). Lastly, higher FA in the right CST was associated with better performance on the CVLT. Marquez de la Plata et al. (2011) found that the FA of the corpus callosum, fornix, cingulum, ILF and IFOF was associated with performance on the CVLT. We did not find any significant associations between WM integrity and cognitive function in the healthy control-only follow up. We did not find any significant associations between WM integrity and cognitive function in the post-acute phase, and we did not find any significant associations between WM integrity and GCS at any phase. Some earlier studies found associations between GCS (or injury severity) and WM integrity (Yuan et al., 2007), but others have failed to detect an association, as we did (Farbota et al., 2012). Our findings linking better WM integrity in the chronic phase to better cognitive performance in TBI demonstrate that DTI metrics can explain some of the variance in outcome after the first year post-injury. There is considerable heterogeneity in recovery and long-term prognosis, and our expectation is that ever-improving DTI technology will help us better understand this heterogeneity and thus implement tailored intervention strategies.

Decreased FA is a hallmark of the neurological disruption following TBI, which can adversely affect some methods of tract reconstruction. The Hough transform method, commonly used by our group as it is a powerful algorithm for fiber tracking in healthy subjects, uses a global function defined on a path to fit tracts through areas that may have low FA (Aganj et al., 2011; Prasad et al., 2011). Even so, it may not be ideal for injured brains. Other methods use the principal eigenvector of the diffusion tensor for reconstruction, which in areas of low FA

means the tract is diverted or dropped. By not being able to track fibers through areas of low FA, these methods are missing the more severely disrupted areas, essentially meaning that statistical comparisons of the resulting data are only comparing the integrity of the less-severely disrupted regions. While autoMATE does use FA to reconstruct tracts, it does not limit the group analyses in the same way previous methods do. In the case of subject data that has areas of low FA that would lead to a premature tract ending, and thus sparse fiber reconstruction, the FA at the location of the warped template point in that subject space is used if the fibers are not detected. This flexibility allows robust group comparisons of WM integrity in a standard space. Thus, autoMATE offers the benefits of tract-based methods in that results are localized in anatomically defined tracts, but it also has the benefits of voxel-based methods, as it can assess integrity even when tract reconstruction is incomplete.

Our study is not without limitations. The results in this paper are restricted to cross-sectional analyses. There is much to be learned from longitudinal analysis, but it also presents a unique set of analytical problems. This will be a focus of future analyses. TBI is a heterogeneous disorder, which has hampered other group analyses. Brain imaging may be used to help identify subgroups of TBI patients that have similar pathobiology, which will hopefully be used to develop targeted therapy. The methods in this paper have the potential to aid in this effort, defining subgroups based on WM disruption patterns. We have shown that chronically those disruptions are associated with poor neurocognitive function. We believe our sample to be representative of the broader population of children with TBI, but only 35% of the eligible patients consented. Most of the participants who chose not to participate did not meet inclusion criteria, such as sufficient English language skills, ADHD or learning disabilities, or lack of interest. The demographic information available from our sample in consistent with the existing epidemiological information on moderate–severe pediatric/adolescent TBI, both in the male to female ratio and in the mechanisms of injury (Keenan and Bratton, 2006). One way to disentangle recruitment bias from confounds in future work is to assess the profile of brain abnormalities in other pediatric cohorts scanned with MRI or DTI, for whom our criteria were not exclusionary. We have such work underway for ADHD as part of the ENIGMA consortium (Hoogman and Mennes, 2014). As this is an on-going study, we expect most children to return for their chronic assessments. Most simply have not reached the chronic time point yet. As with any study, we face issues of attrition, and we have lost some subjects between their post-acute and chronic time points. 1 subject was indeed scanned chronically, but data quality issues (artifacts) meant we could not include them, 3 subjects only received functional MRI at the chronic time point, 2 subjects were brought back

for the chronic assessment but not scanned, 3 had braces at time 2, 3 were disqualified at time 2 for ADHD or LD (learning disability), 1 family refused to return, 2 moved out of state, 1 was referred by his doctor to the study and had already missed the post-acute window, and 8 were lost to follow-up, meaning they could have moved, changed their phone number, or simply stopped returning our calls. There was no systematic reason for the non-returns.

In some studies of this kind, it is common to include orthopedic injury subjects as controls. This is especially helpful for studies investigating the psychosocial and cognitive outcomes where there may be a concern about pre-injury level of function. There may be some groups that arguably put themselves at higher risk for TBI because of their choices and actions, such as athletes and military personnel. This is a particular concern for groups who incur TBI related to activities that they choose to do that put them at higher risk. This is less of an issue for our pediatric cohort, although it cannot be ruled out. Most of participants sustained TBI through motor vehicle accidents (as a pedestrian or passenger) or falls from bikes, scooters, and skateboards (accounting for 75% of our participants). We consider these events to be somewhat random, and would be surprised if there was any biologically identifiable factor that predisposed individuals to experiencing these, in such a way as to influence our results here. We took measures to recruit healthy controls from the same community sample as the TBI participants to limit any bias, such as public school and community based programs from the same communities as the TBI subjects.

In this study, we examined pediatric TBI patients at two time-points across the first year and a half post-injury. We did not detect differences between TBI patients and controls post-acutely. In the chronic phase, differences between the groups were more extensive, and MD and RD were better indicators of disruption. Prior work has similarly shown progressive WM disruptions over the first year post-injury (Bendlin et al., 2008; Wu et al., 2010), and other researchers have similarly found that the diffusivity metrics that are best for detecting the disruption of TBI change between the post-acute and chronic phases (Wilde et al., 2012). Perhaps our finding more group differences in the chronic phase reflects the injury heterogeneity dominating the analyses post-acutely, while chronically the progressive, widespread WM damage plays a more major role. One theorized mechanism of TBI that could lead to this is diaschisis, where disruption occurs in one area of the brain distant, but connected to the damaged area (Feeney and Baron, 1986). Alternatively, this might reflect the late effects of inflammatory processes (Lenzlinger et al., 2001). Lower FA, higher MD and higher RD all suggest that TBI leads to myelin damage, rather than axonal damage, which other researchers have suggested as well (Farbota et al., 2012; Caeyenberghs et al., 2011; Dinkel et al., 2014; Ewing-Cobbs et al., 2008; Oni et al., 2010), although some have found evidence of axonal damage (Sidaros et al., 2008; Caeyenberghs et al., 2010). We were also able to link disruptions in WM integrity to impaired cognitive function in the TBI patients. Outcome following TBI is quite heterogeneous and there is a considerable amount of the variance that is currently unexplained. DTI methods have proven to be sensitive and powerful tools in the study of TBI. We expect they will also prove useful in the effort to explain some of this variance and tailor interventions.

Acknowledgements

References

Aganj, I., Lenglet, C., Jahanshad, N., Yacoub, E., Harel, N., Thompson, P.M., Sapiro, G., 2011. A Hough transform global probabilistic approach to multiple-subject diffusion MRI tractography. Med. Image Anal. 15 (4), 414–425. http://dx.doi.org/10.1016/j.media.2011.01.00321376655.

Avants, B.B., Tustison, N.J., Song, G., Cook, P.A., Klein, A., Gee, J.C., 2011. A reproducible evaluation of ANTs similarity metric performance in brain image registration. Neuroimage 54 (3), 2033–2044. http://dx.doi.org/10.1016/j.neuroimage.2010.09.02520851191.

Barzó, P., Marmarou, A., Fatouros, P., Hayasaki, K., Corwin, F., 1997. Contribution of vasogenic and cellular edema to traumatic brain swelling measured by diffusion-weighted imaging. J. Neurosurg. 87 (6), 900–907. http://dx.doi.org/10.3171/jns.1997.87.6.09009384402.

Bendlin, B.B., Ries, M.L., Lazar, M., Alexander, A.L., Dempsey, R.J., Rowley, H.A., Sherman, J.E., Johnson, S.C., 2008. Longitudinal changes in patients with traumatic brain injury assessed with diffusion-tensor and volumetric imaging. Neuroimage 42 (2), 503–514. http://dx.doi.org/10.1016/j.neuroimage.2008.04.25418556217.

Benjamini, Y., Hochberg, Y., 1995. Controlling the false discovery rate: a practical and powerful approach to multiple testing. J. R. Stat. Soc. B. 57 (1), 289–300.

Budde, M.D., Janes, L., Gold, E., Turtzo, L.C., Frank, J.A., 2011. The contribution of gliosis to diffusion tensor anisotropy and tractography following traumatic brain injury: validation in the rat using Fourier analysis of stained tissue sections. Brain J. Neurol. 134 (8), 2248–2260. http://dx.doi.org/10.1093/brain/awr16121764818.

Büki, A., Povlishock, J.T., 2006. All roads lead to disconnection?—traumatic axonal injury revisited. Acta Neurochir. 148 (2), 181–194. http://dx.doi.org/10.1007/s00701-005-0674-416362181.

Caeyenberghs, K., Leemans, A., Coxon, J., Leunissen, I., Drijkoningen, D., Geurts, M., Gooijers, J., Michiels, K., Sunaert, S., Swinnen, S.P., 2011. Bimanual coordination and corpus callosum microstructure in Young adults with traumatic brain injury: a diffusion tensor imaging study. J. Neurotrauma 28 (6), 897–913. http://dx.doi.org/10.1089/neu.2010.172121501046.

Caeyenberghs, K., Leemans, A., Geurts, M., Taymans, T., Vander Linden, C., Smits-Engelsman, B.C., Sunaert, S., Swinnen, S.P., 2010. Brain-behavior relationships in young traumatic brain injury patients: fractional anisotropy measures are highly correlated with dynamic visuomotor tracking performance. Neuropsychologia 48 (5), 1472–1482. http://dx.doi.org/10.1016/j.neuropsychologia.2010.01.01720117121.

Catani, M., Allin, M.P., Husain, M., Pugliese, L., Mesulam, M.M., Murray, R.M., Jones, D.K., 2007. Symmetries in human brain language pathways correlate with verbal recall. Proc. Natl. Acad. Sci. U.S.A 104 (43), 17163–17168. http://dx.doi.org/10.1073/pnas.070211610417939998.

Catani, M., Dell'acqua, F., Bizzi, A., Forkel, S.J., Williams, S.C., Simmons, A., Murphy, D.G., Thiebaut de Schotten, M., 2012. Atlas of Human Brain Connections. Oxford University Press http://dx.doi.org/10.1016/j.cortex.2012.07.00122995574.

Delis, D.C., Kaplan, E., Kramer, J.H., 2001. Delis–Kaplan Executive Function System (D-KEFS). Psychological Corporation.

Delis, D.C., Kramer, J.H., Kaplan, E., Ober, A., 1994. California Verbal Learning Test-Children's Version (CVLT-C). ManualPsychological Corporation, San Antonio, TX.

Dinkel, J., Drier, A., Khalilzadeh, O., Perlbarg, V., Czernecki, V., Gupta, R., Gomas, F., Sanchez, P., Dormont, D., Galanaud, D., Stevens, R.D., Puybasset, L., NICER Consortium, 2014. Long-term white matter changes after severe traumatic brain injury: a 5-year prospective cohort. A.J.N.R. Am. J. Neuroradiol. 35 (1), 23–29. http://dx.doi.org/10.3174/ajnr.A361623846796.

Ewing-Cobbs, L., Prasad, M.R., Swank, P., Kramer, L., Cox, C.S., Fletcher, J.M., Barnes, M., Zhang, X., Hasan, K.M., 2008. Arrested development and disrupted callosal microstructure following pediatric traumatic brain injury: relation to neurobehavioral outcomes. Neuroimage 42 (4), 1305–1315. http://dx.doi.org/10.1016/j.neuroimage.2008.06.03118655838.

Farbota, K.D., Bendlin, B.B., Alexander, A.L., Rowley, H.A., Dempsey, R.J., Johnson, S.C., 2012. Longitudinal diffusion tensor imaging and neuropsychological correlates in traumatic brain injury patients. Front. Hum. Neurosci. 6, 160.

Feeney, D.M., Baron, J.-C., 1986. Diaschisis. Stroke 17 (5), 817–830. http://dx.doi.org/10.1161/01.STR.17.5.8173532434.

Greenberg, G., Mikulis, D.J., Ng, K., DeSouza, D., Green, R.E., 2008. Use of diffusion tensor imaging to examine subacute white matter injury progression in moderate to severe traumatic brain injury. Arch Phys Med Rehabil 89 (12 Suppl), S45–S50. http://dx.doi.org/10.1016/j.apmr.2008.08.21119081441.

Hoogman, M., Mennes, M., Zwiers, M., E.A.w. group, 2014. Brain Structure and ADHD Across the Life Span: An ENIGMA Collaboration. OHBM, Hamburg, Germany.

Hua, X., Leow, A.D., Parikshak, N., Lee, S., Chiang, M.-C., Toga, A.W., Jack Jr, C.R., Weiner, M.W., Thompson, P.M., Alzheimer's Disease Neuroimaging Initiative, 2008. Tensor-based morphometry as a neuroimaging biomarker for Alzheimer's disease: an MRI study of 676 AD, MCI, and normal subjects. Neuroimage 43 (3), 458–469. http://dx.doi.org/10.1016/j.neuroimage.2008.07.01318691658.

Hulkower, M.B., Poliak, D.B., Rosenbaum, S.B., Zimmerman, M.E., Lipton, M.L., 2013. A decade of DTI in traumatic brain injury: 10 years and 100 articles later. A.J.N.R. Am. J. Neuroradiol. 34, 2064–2074. http://dx.doi.org/10.3174/ajnr.A339523306011.

Jin, Y., Shi, Y., Zhan, L., de Zubicaray, G.I., McMahon, K.L., Martin, N.G., Wright, M.J., Thompson, P.M., 2013. Labeling white matter tracts in HARDI by fusing multiple tract atlases with applications to genetics. Proc. IEEE Int. Symp. Biomed. Imaging 2013, 512–515. http://dx.doi.org/10.1109/ISBI.2013.655652425419442.

Jin, Y., Shi, Y., Zhan, L., Gutman, B.A., de Zubicaray, G.I., McMahon, K.L., Wright, M.J., Toga, A.W., Thompson, P.M., 2014. Automatic clustering of white matter fibers in brain diffusion MRI with an application to genetics. Neuroimage 100, 75–90. http://dx.doi.org/10.1016/j.neuroimage.2014.04.04824821529.

Jin, Y., Shi, Y., Zhan, L., Li, J., De Zubicaray, G.I., Mc Mahon, K.L., Martin, N.G., Wright, M.J., Thompson, P.M., 2012. Automatic population HARDI white matter tract clustering by label fusion of multiple tract atlases. Multimodal Brain Image Analysis. Springer Berlin Heidelberg, pp. 147–156.

Keenan, H.T., Bratton, S.L., 2006. Epidemiology and outcomes of pediatric traumatic brain injury. Dev. Neurosci. 28 (4–5), 256–263. http://dx.doi.org/10.1159/00009415216943649.

Kinnunen, K.M., Greenwood, R., Powell, J.H., Leech, R., Hawkins, P.C., Bonnelle, V., Patel, M.C., Counsell, S.J., Sharp, D.J., 2010. White matter damage and cognitive impairment after traumatic brain injury. Brain awq347.

Kochunov, P., Williamson, D.E., Lancaster, J., Fox, P., Cornell, J., Blangero, J., Glahn, D.C., 2012. Fractional anisotropy of water diffusion in cerebral white matter across the lifespan. Neurobiol. Aging 33, 9–20. http://dx.doi.org/10.1016/j.neurobiolaging.2010.01.01420122755.

Lee, H., Wintermark, M., Gean, A.D., Ghajar, J., Manley, G.T., Mukherjee, P., 2008. Focal lesions in acute mild traumatic brain injury and neurocognitive outcome: CT versus 3T MRI. J. Neurotrauma 25 (9), 1049–1056. http://dx.doi.org/10.1089/neu.2008.056618707244.

Lenzlinger, P.M., Morganti-Kossmann, M.-C., Laurer, H.L., McIntosh, T.K., 2001. The duality of the inflammatory response to traumatic brain injury. Mol. Neurobiol. 24 (1–3), 169–181. http://dx.doi.org/10.1385/MN:24:1-3:16911831551.

Levin, H.S., Wilde, E.A., Chu, Z., Yallampalli, R., Hanten, G.R., Li, X., Chia, J., Vasquez, A.C., Hunter, J.V., 2008. Diffusion tensor imaging in relation to cognitive and functional outcome of traumatic brain injury in children. J. Head Trauma Rehabil. 23 (4), 197–208. http://dx.doi.org/10.1097/01.HTR.0000327252.54128.7c18650764.

Mac Donald, C.L., Dikranian, K., Song, S.K., Bayly, P.V., Holtzman, D.M., Brody, D.L., 2007. Detection of traumatic axonal injury with diffusion tensor imaging in a mouse model of traumatic brain injury. Exp. Neurol. 205 (1), 116–131. http://dx.doi.org/10.1016/j.expneurol.2007.01.03517368446.

Marmarou, A., Signoretti, S., Fatouros, P.P., Portella, G., Aygok, G.A., Bullock, M.R., 2006. Predominance of cellular edema in traumatic brain swelling in patients with severe head injuries. J. Neurosurg. 104 (5), 720–730. http://dx.doi.org/10.3171/jns.2006.104.5.72016703876.

Marquez de la Plata, C.D., Yang, F.G., Wang, J.Y., Krishnan, K., Bakhadirov, K., Paliotta, C., Aslan, S., Devous, M.D., Moore, C., Harper, C., McColl, R., Munro Cullum, C., Diaz-Arrastia, R., 2011. Diffusion tensor imaging biomarkers for traumatic axonal injury: analysis of three analytic methods. J. Int. Neuropsychol. Soc. JINS 17 (1), 24–35. http://dx.doi.org/10.1017/S1355617710001189121070694.

Oni, M.B., Wilde, E.A., Bigler, E.D., McCauley, S.R., Wu, T.C., Yallampalli, R., Chu, Z., Li, X., Hunter, J.V., Vasquez, A.C., Levin, H.S., 2010. Diffusion tensor imaging analysis of frontal lobes in pediatric traumatic brain injury. J. Child Neurol. 25 (8), 976–984. http://dx.doi.org/10.1177/088307380935603420332386.

Pal, D., Gupta, R.K., Agarwal, S., Yadav, A., Ojha, B.K., Awasthi, A., Rathore, R.K., Pandey, C.M., Narayana, P.A., 2012. Diffusion tensor tractography indices in patients with frontal lobe injury and its correlation with neuropsychological tests. Clin. Neurol. Neurosurg. 114 (6), 564–571. http://dx.doi.org/10.1016/j.clineuro.2011.12.00222209144.

Prasad, G., Jahanshad, N., Aganj, I., Lenglet, C., Sapiro, G., Toga, A.W., Thompson, P.M., 2011. Atlas-based fiber clustering for multi-subject analysis of high angular resolution diffusion imaging tractography. IEEE 1–5.

Sidaros, A., Engberg, A.W., Sidaros, K., Liptrot, M.G., Herning, M., Petersen, P., Paulson, O.B., Jernigan, T.L., Rostrup, E., 2008. Diffusion tensor imaging during recovery from severe traumatic brain injury and relation to clinical outcome: a longitudinal study. Brain J. Neurol. 131 (2), 559–572. http://dx.doi.org/10.1093/brain/awm29418083753.

Teasdale, G., Murray, G., Parker, L., Jennett, B., 1979. Adding up the Glasgow coma score. Acta Neurochir. Suppl. 28 (1), 13–16290137.

Thomason, M.E., Thompson, P.M., 2011. Diffusion imaging, white matter, and psychopathology. Annu. Rev. Clin. Psychol. 7, 63–85. http://dx.doi.org/10.1146/annurev-clinpsy-032210-10450721219189.

Wechsler, D., 2003. Wechsler Intelligence Scale for Children—Fourth Edition (WISC-IV). The Psychological Corporation, San Antonio, TX.

Wilde, E.A., Ayoub, K.W., Bigler, E.D., Chu, Z.D., Hunter, J.V., Wu, T.C., McCauley, S.R., Levin, H.S., 2012. Diffusion tensor imaging in moderate-to-severe pediatric traumatic brain injury: changes within an 18 month post-injury interval. Brain Imaging Behav. 6 (3), 404–416. http://dx.doi.org/10.1007/s11682-012-9150-y22399284.

Wilde, E.A., Chu, Z., Bigler, E.D., Hunter, J.V., Fearing, M.A., Hanten, G., Newsome, M.R., Scheibel, R.S., Li, X., Levin, H.S., 2006. Diffusion tensor imaging in the corpus callosum in children after moderate to severe traumatic brain injury. J. Neurotrauma 23 (10), 1412–1426. http://dx.doi.org/10.1089/neu.2006.23.141217020479.

Wilde, E.A., McCauley, S.R., Hunter, J.V., Bigler, E.D., Chu, Z., Wang, Z.J., Hanten, G.R., Troyanskaya, M., Yallampalli, R., Li, X., Chia, J., Levin, H.S., 2008. Diffusion tensor imaging of acute mild traumatic brain injury in adolescents. Neurology 70 (12), 948–955. http://dx.doi.org/10.1212/01.wnl.0000305961.68029.5418347317.

Wilde, E.A., Newsome, M.R., Bigler, E.D., Pertab, J., Merkley, T.L., Hanten, G., Scheibel, R.S., Li, X., Chu, Z., Yallampalli, R., Hunter, J.V., Levin, H.S., 2011. Brain imaging correlates of verbal working memory in children following traumatic brain injury. Int. J. Psychophysiol. 82 (1), 86–96. http://dx.doi.org/10.1016/j.ijpsycho.2011.04.00621565227.

Wozniak, J.R., Krach, L., Ward, E., Mueller, B.A., Muetzel, R., Schnoebelen, S., Kiragu, A., Lim, K.O., 2007. Neurocognitive and neuroimaging correlates of pediatric traumatic brain injury: a diffusion tensor imaging (DTI) study. Arch. Clin. Neuropsychol. 22 (5), 555–568. http://dx.doi.org/10.1016/j.acn.2007.03.00417446039.

Wu, T.C., Wilde, E.A., Bigler, E.D., Li, X., Merkley, T.L., Yallampalli, R., McCauley, S.R., Schnelle, K.P., Vasquez, A.C., Chu, Z., Hanten, G., Hunter, J.V., Levin, H.S., 2010. Longitudinal changes in the corpus callosum following pediatric traumatic brain injury. Dev. Neurosci. 32, 361–373. http://dx.doi.org/10.1159/00031705820948181.

Xu, J., Rasmussen, I.-A., Lagopoulos, J., Håberg, A., 2007. Diffuse axonal injury in severe traumatic brain injury visualized using high-resolution diffusion tensor imaging. J. Neurotrauma 24 (5), 753–765. http://dx.doi.org/10.1089/neu.2006.020817518531.

Yallampalli, R., Wilde, E.A., Bigler, E.D., McCauley, S.R., Hanten, G., Troyanskaya, M., Hunter, J.V., Chu, Z., Li, X., Levin, H.S., 2013. Acute white matter differences in the fornix following mild traumatic brain injury using diffusion tensor imaging. J Neuroimaging 23 (2), 224–227. http://dx.doi.org/10.1111/j.1552-6569.2010.00537.x21988147.

Yuan, W., Holland, S.K., Schmithorst, V.J., Walz, N.C., Cecil, K.M., Jones, B.V., Karunanayaka, P., Michaud, L., Wade, S.L., 2007. Diffusion tensor MR imaging reveals persistent white matter alteration after traumatic brain injury experienced during early childhood. A.J.N.R. Am. J. Neuroradiol. 28 (10), 1919–1925. http://dx.doi.org/10.3174/ajnr.A069817905895.

Zhang, Y., Zhang, J., Oishi, K., Faria, A.V., Jiang, H., Li, X., Akhter, K., Rosa-Neto, P., Pike, G.B., Evans, A., Toga, A.W., Woods, R., Mazziotta, J.C., Miller, M.I., van Zijl, P.C., Mori, S., 2010a. Atlas-guided tract reconstruction for automated and comprehensive examination of the white matter anatomy. Neuroimage 52 (4), 1289–1301. http://dx.doi.org/10.1016/j.neuroimage.2010.05.04920570617.

Zhang, Y., Zhang, J., Oishi, K., Faria, A.V., Jiang, H., Li, X., Akhter, K., Rosa-Neto, P., Pike, G.B., Evans, A., Toga, A.W., Woods, R., Mazziotta, J.C., Miller, M.I., van Zijl, P.C., Mori, S., 2010b. Atlas-guided tract reconstruction for automated and comprehensive examination of the white matter anatomy. Neuroimage 52 (4), 1289–1301. http://dx.doi.org/10.1016/j.neuroimage.2010.05.04920570617.